



## DISCRETIZED GLOBAL OPERATORS AND ALL-SOURCE GREEN'S FUNCTIONS OF SHALLOW WATER EQUATIONS FOR REAL-TIME SIMULATIONS OF TSUNAMI ARRIVALS

Zhigang Xu<sup>1</sup>

### ABSTRACT

Global difference operators are constructed to recast the linear shallow water equations in a matrix form. The matrix form allows for a straight forward switch from the traditional single-source Green's function to a new type of Green's function, an all-source Green's function (ASGF). The values of the ASGF in tsunami real-time simulations and in inferring initial forcing are discussed. Also presented are implementation details for a demonstrative real-time system to simulate tsunami arrivals at points of interest from anywhere in the North Atlantic Ocean.

Keywords: shallow water equations, global difference operators, sparse matrices, all-source Green's functions, real-time tsunami simulations.

### Introduction

A tsunami is disastrous, yet fortunately its propagation in deep water (>50m, Shuto 1991) obeys the linear long wave dynamics very well. This means that Green's functions can come to help for a quick real-time simulations to win life saving time. This is because Green's functions can be pre-calculated and can be linearly combined to instantaneously yield the ocean's response to an eventual tsunami forcing. Traditionally a Green's function is defined as a system wise response to a delta-impulse acting at one point. However a tsunami is rarely triggered at one point. A logical extension is to pre-calculate a group of Green's functions corresponding to a group of points in a pre-assumed tsunami source region. Nevertheless when a future tsunami happens outside of the pre-assumed source region, the pre-calculated Green's functions will not be helpful.

Xu (2007) proposed a new type of Green's function, all-source Green's function (ASGF), which focuses on a receiver point, regarding all the model grid points as the potential source points. The computational cost for calculating an ASGF is the same as that for an SSGF, however the ASGF provides a thorough preparedness for a point of interest (POI) against all possible sources. Xu recast the linear shallow water equations in matrix form with a few discretized global operators as sub-matrices. This led him to calculate the ASGFs in a straight

---

<sup>1</sup> Modeling and Operational Oceanography, Canadian Hydrographic Service, Maurice Lamontagne Institute, Fisheries and Oceans Canada, Mon-Joli, Quebec, Canada, G5H 3Z4

forward manner. Based on the ASGF, he further proposed and demonstrated 1) a real-time simulation system of tsunami arrivals from anywhere in the North Atlantic Ocean, 2) a tsunami *arrival time* chart at a POI, as against the traditional tsunami *travel time* chart out of a source point, and 3) a tsunami gain chart, where a gain is defined as the maximum amplitude during 12 hours relative to the source amplitude. However for that paper he omitted on how to construct the discretized global operators and how to recast the linear shallow water equations in a single matrix equation. This paper will focus on this important aspect. It will also detail the implementation of the North Atlantic Ocean real-time tsunami simulation system.

### Linear Shallow Water Equations in Matrix Form

The following continuous form of the linearized shallow water partial differential equations in spherical coordinates are chosen for modeling the tsunami propagations in deep waters mounted on the rotating Earth with frictions on the seabed,

$$\frac{\partial \eta}{\partial t} = -\frac{1}{R \cos \varphi} \left( \frac{\partial hu}{\partial \lambda} + \frac{\partial hv}{\partial \varphi} \right) \quad (1)$$

$$\frac{\partial u}{\partial t} = -\frac{g}{R \cos \varphi} \frac{\partial \eta}{\partial \lambda} + fv - \frac{\kappa u}{h} \quad (2)$$

$$\frac{\partial v}{\partial t} = -\frac{g}{R} \frac{\partial \eta}{\partial \varphi} - fu - \frac{\kappa v}{h} \quad (3)$$

where the notations are explained in the table below:

$\lambda, \varphi, t$	Longitude, latitude, and time variables respectively
$\eta, u, v,$	Sea surface elevation, depth averaged velocities in longitudinal and latitudinal directions
$f, g, R,$	Coriolis parameter, gravity acceleration, and the Earth' mean radius.
$h, \kappa$	Water depth and bottom frictional coefficients, $\kappa = 2.4 \times 10^{-3}$ m/s (Heaps, 1969).

Table 1 Notations in the linear shallow water equations.

The lateral boundary conditions are no normal flows at the solid boundaries and Sommerfeld (1949) radiation conditions at open water boundaries. The no-normal flows at the solid boundaries result in the following geostrophic flow constraints:

$$fv = \frac{g}{R \cos \varphi} \frac{\partial \eta}{\partial \lambda} \quad \text{at east-west solid boundaries, where } u \equiv 0 \quad (4)$$

$$fu = -\frac{g}{R} \frac{\partial \eta}{\partial \varphi} \quad \text{at south-north solid boundaries, where } v \equiv 0 \quad (5)$$

where the east-west solid boundaries mean those solid boundaries whose normal directions are in the longitudinal directions, and the south-north solid boundaries mean those solid boundaries

whose normal direction in the latitudinal directions. Along these solid boundaries, either  $u \equiv 0$  or  $v \equiv 0$ , resulting in the geostrophic relationship as appropriate boundary conditions. Note the lateral frictional effects are not considered here, which means flow can slip against the walls.

The general form of the Sommerfeld radiation boundary conditions is

$$\frac{\partial p}{\partial t} + c \frac{\partial p}{\partial n} = 0 \quad (6)$$

where  $p$  may represent  $u$  or  $\eta$  if they are not collocated on a computational grid or both if they are collocated, and  $c$  is a phase speed, and  $\partial n$  means an infinitesimal line segment outward normal to the open boundaries. Chapman (1985) discussed various forms of  $c$  and compared their numerical effects on the quality of the model solutions inside of the model domain. For this study,  $c = \sqrt{gh}$  is taken.

The spatial differential operators,  $\partial/\partial x$  and  $\partial/\partial y$ , can be approximated by spatial difference operators  $\Delta/\Delta x$ , and  $\Delta/\Delta y$ . The latter are usually treated as point-wise operators, which means, for example, when  $\Delta/\Delta x$ , operates on a local point  $u_i$ , it only produces a local result for that point,  $\Delta u_{ij}/\Delta x = (u_{i,j+1} - u_{i,j})/\Delta x$ . This study takes a global operator approach. This means that all the point-wise operators are assembled first into a single matrix before any operations on the solution vector take place. The ASGF proposed by Xu (2007) was based on the global operator approach. How to build the global operators was not reported in that paper. The following discussion shows how they can be built.

For example, in place of continuous form of  $\partial(hu)/\partial x$ , there will be  $\mathbb{D}IV_x(hu)$ , where the  $hu$  in the second expression is a column vector as a collection of the discretized version of the continuous version of  $hu$  in the first expression. Here the notation  $\mathbb{D}IV_x$  in double struck letters stands for a single sparse matrix, when it operates on the column vector  $hu$ , it produces the mass divergence in the  $x$ -direction at all the elevation grid points in the entire model domain. Thus, the matrix  $\mathbb{D}IV_x$  is a global operator. Note that the notation  $x$  and  $y$  does not necessary imply a Cartesian coordinate system. In this paper they should be understood as synonyms to longitudes and latitudes. Because each node is connected with only a few neighbor nodes, the global operator is a highly sparse matrix and should be accommodated by a sparse matrix storage scheme.

With the global operators, one can approximate Eqs. (1), (2) and (3), together with all the appropriate lateral boundary conditions, by a single matrix equation as below,

$$\frac{\partial}{\partial t} \begin{bmatrix} \eta \\ hu \\ hv \end{bmatrix} = \begin{bmatrix} 0 + \mathbb{O}B_\eta & -\mathbb{D}IV_x & -\mathbb{D}IV_y \\ -gh\mathbb{G}RAD_x & \mathbb{S}N_x f - \kappa h^{-1} + \mathbb{O}B_u & (\mathbb{I} - \mathbb{W}E_x)f \\ -gh\mathbb{G}RAD_y & (\mathbb{S}N_y - \mathbb{I})f & -\mathbb{W}E_y f - \kappa h^{-1} + \mathbb{O}B_v \end{bmatrix} \begin{bmatrix} \eta \\ hu \\ hv \end{bmatrix} \quad (7)$$

where different operators (sub-matrices) are explained in Table 2 below. The geostrophic relations at the solid boundaries conditions shown in Eqs. (4) and (5) are implemented through the four solid boundary operators,  $\mathbb{S}N_x$ ,  $\mathbb{S}N_y$ ,  $\mathbb{W}E_x$ , and  $\mathbb{W}E_y$ , which give the Coriolis force

upon operating on  $hu$  and  $hv$  at all the velocity points along the coasts, and through the two pressure gradient operators,  $\text{GRAD}_x$  and  $\text{GRAD}_y$ , which, upon operating on the elevation vector  $\eta$ , produce the pressure gradient forces at all the velocity points globally including those along the coasts. Here a west solid boundary does not necessarily mean the far west boundary in a model domain. To cover arbitrary costal and island geometries, a west solid boundary is defined as any solid boundary where there is water to its east. The east, north and south solid boundaries are defined similarly.

$0$	A zero-matrix of size $m \times m$ where $m$ is the number of total elevation grid points.
$\text{DIV}_x, \text{DIV}_y$	Matrix operators, of sizes $m \times n$ , for the mass divergences in $x$ - and $y$ -directions, where $n$ stands for the number of the velocity grid points.
$\text{GRAD}_x, \text{GRAD}_y$	Sea surface gradient operators in $x$ - and $y$ - directions, and of sizes $n \times m$ .
$\text{SN}_x, \text{SN}_y$	Two south-north solid boundary operators in $x$ - and $y$ -directions respectively, and of sizes $n \times m$ .
$\text{WE}_x, \text{WE}_y$	Two west-east solid boundary operators in $x$ - and $y$ -directions respectively, and of sizes $n \times m$ .
$\text{OB}_\eta, \text{OB}_u, \text{OB}_v$	Three open boundary operators for $\eta$ -, $u$ - and $v$ - points respectively. The size of $\text{OB}_\eta$ is $m \times m$ and the sizes of $\text{OB}_u$ and $\text{OB}_v$ are $n \times n$ .
$h, \kappa$	Diagonal matrices for the spatial varying water depths and bottom frictions respectively. Their sizes are $n \times n$ . For this study, $\kappa = 2.4 \times 10^{-3}\text{I}$ .
$f, \text{I}$	A diagonal matrix for the spatial varying Coriolis parameter, and an identical matrix; their sizes are $n \times n$ .
$g$	A scalar for the earth's gravity acceleration.

Table 2. An operator table. The  $x$ - and  $y$ -directions as well as the  $x$  and  $y$  subscripts in the table do not necessary imply a Cartesian coordinate system being used. In this study, the  $x$  and  $y$  should be regarded as synonyms to longitudinal and latitudinal coordinates.

The open water boundary conditions are implemented through the operators  $\text{OB}_\eta$ ,  $\text{OB}_u$ , and  $\text{OB}_v$ . Note that these open boundary operators have non-zero elements only at rows corresponding to the open boundary nodes, and that they are mutual exclusive with the other operators in that when  $\text{OB}_u$ , for example, has non-zero rows, all the other operators and sub-matrices in the second line of Eq. (7) will have all zero elements in the corresponding rows.

Now the continuous shallow water PDEs have been semi-discretized, by which it is meant that they are still continuous in time. All the dynamics and the lateral conditions and arbitrary geometry and have been encapsulated into the coefficient matrix. For this reason, it may be referred as the dynamic matrix. The dynamics matrix consists of  $3 \times 3$  sub-matrices. The roles and meaning of the sub-matrices should be self evident through their descriptive notations

and their positions corresponding to the positions of the terms in the shallow water equations in continuous form. If one zeros-out subs(2:3,2:3), which mean the sub-matrices from the second to third rows and from the second to the third columns, the dynamics is reduced to the wave dynamics on a non-rotating frame, which seems also a common choice in tsunami research.

So far, no commitment has been made to a particular type of spatial grid, nor to a special time discretization scheme. Thus, one is free to choose a combination of spatial-time discretization schemes in forming a stable and good quality numerical model. This study adopts the same staggered grid as that used by Heaps (1969), where the elevation points are located in the middle of cells and velocities points are collocated on the corners of the cells (See **Error! Reference source not found.**). Arakawa and Lamb (1977) catalogued this type of grid as B-grid. The grid is constructed such that all the elevation points are the interior points. This means that the Sommerfeld radiation condition is only applied to  $u$ - and  $v$ - open water boundary points, and hence  $\mathbb{O}\mathbb{B}_\eta$  can be entirely removed from Eq. (7). With the boundary operators presented in the matrix equation, one can easily switch between different types of boundary conditions.

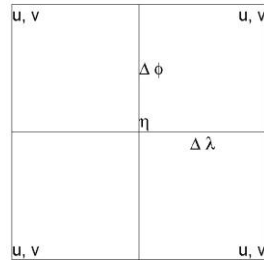


Figure 1. The same staggered grid as that in Heaps (1969) is used for this study. It is also known as Arakawa B-grid.

Further numerical details can be found in Heaps (1969) with one exception: In treating the pressure gradient along a lateral boundary, Heaps required that there were at least two elevation points next and perpendicular to the boundary. He constructed an *ad-hoc* grid for modeling storm surges the North Sea so that such requirement was always met. In covering a general geometry, especially with a fine resolution, it is not always possible to have at least two such interior elevation points. There are many narrow channels/bays which can only hold one such elevation point. Thus this study uses only one elevation node in treating the pressure gradient along a coast. The existence of at least one such elevation node is guaranteed, since otherwise the channel/bay would be a solid land. It is in the author's plan to publish elsewhere a set of Matlab functions to calculate the global operators.

With a simple forward difference scheme in time, Eq. (7) can be further approximated by

$$\begin{bmatrix} \eta \\ hu \\ hv \end{bmatrix}^{(k+1)} = B \begin{bmatrix} \eta \\ hu \\ hv \end{bmatrix}^{(k)} \quad (8)$$

where  $B = I + \Delta t M$  in which  $M$  stands for the dynamic matrix in Eq. (7) for brevity,  $\Delta t$  is the time step,  $I$  is an identical matrix, the superscript  $k$  inside the parentheses indicate the time steps. To stabilize the numerical scheme, Heaps (1969) used the most updated variables in evaluating

the right hand side of Eq. (8). Thus Eq. (8) should be modified as

$$\begin{bmatrix} \eta \\ hu \\ hv \end{bmatrix}^{(k+1)} = \begin{bmatrix} B_{11} & B_{12} & B_{13} \\ 0 & B_{22} & B_{23} \\ 0 & 0 & B_{33} \end{bmatrix} \begin{bmatrix} \eta \\ hu \\ hv \end{bmatrix}^{(k)} + \begin{bmatrix} 0 & 0 & 0 \\ B_{21} & 0 & 0 \\ B_{31} & B_{32} & 0 \end{bmatrix} \begin{bmatrix} \eta \\ hu \\ hv \end{bmatrix}^{(k+1)} \quad (9)$$

The above equation can be further cast as

$$\begin{bmatrix} \eta \\ hu \\ hv \end{bmatrix}^{(k+1)} = \mathbf{A} \begin{bmatrix} \eta \\ hu \\ hv \end{bmatrix}^{(k)} \quad (10)$$

where

$$\mathbf{A} = \begin{bmatrix} I & 0 & 0 \\ -B_{21} & I & 0 \\ -B_{31} & -B_{32} & I \end{bmatrix}^{-1} \begin{bmatrix} B_{11} & B_{12} & B_{13} \\ 0 & B_{22} & B_{23} \\ 0 & 0 & B_{33} \end{bmatrix} \quad (11)$$

The inversion of the first factor matrix is easy to calculate, since no actual inversion needs to be performed. It is,

$$\begin{bmatrix} I & 0 & 0 \\ -B_{21} & I & 0 \\ -B_{31} & -B_{32} & I \end{bmatrix}^{-1} = \begin{bmatrix} I & 0 & 0 \\ B_{21} & I & 0 \\ B_{32}B_{21} + B_{31} & B_{32} & I \end{bmatrix} \quad (12)$$

Thus,  $\mathbf{A}$  can be finally expressed as

$$\mathbf{A} = \begin{bmatrix} B_{11} & B_{12} & B_{13} \\ B_{21}B_{11} & B_{21}B_{12} + B_{22} & B_{21}B_{13} + B_{33} \\ \beta B_{11} & \beta B_{12} + B_{32}B_{22} & \beta B_{13} + B_{32}B_{23} + B_{33} \end{bmatrix} \quad (13)$$

where  $\beta = B_{32}B_{21} + B_{31}$ . Since the dynamics matrix  $\mathbf{M}$  is now contained in matrix  $\mathbf{A}$ , the latter may be also called the dynamics matrix. It is a global operator too, a giant one containing all the others. When it operates the current ocean state vector,  $[\eta \ hu \ hv]^T$ , it updates the state vector to the next time step. For this reason, it may be also called the update operator/matrix.

Heaps (1969) suggested the time step as  $\Delta t = r \ 2 \ \min(R \ \Delta \phi, R \ \cos \phi \ \Delta \lambda) / \sqrt{gh}$  where  $r$  is a lower bound to bring the time step  $\Delta t$  within the maximum value allowed by the CFL condition. In this study,  $r$  is set as 0.99.

### Single-Source Green's Functions *versus* All-Source Green's Functions

With Eq. (10), one can now put the SSGF and the ASGF on the same footing for comparison. This helps to see clearly the logical development from the former to the latter, and their different focuses and features as well.

## Single-Source Green's Function (SSGF)

Traditionally a Green's function is mathematically defined as the response of a linear dynamic system to a delta impulse acting on a spatial point, and computationally calculated as model's solution to a unit impulse acting on a model grid point. For the setting here, this means that

```
SSGF(:, kmax)=zeros(m+2*n,1); % pre-allocate memories
SSGF(i,1)=1 ; % a unit source at i'th grid point.

for k=2:kmax % time stepping
    SSGF(:,k)=A*SSGF(:,k-1);
end
```

where  $\mathbf{A}$  is specified by Eq. (13). Thus, a Green's function can be pre-calculated before any real tsunami happens. When a future disturbance indeed happens at the  $i$ 'th grid point, a scale up or down of the pre-calculated Green's function can immediately give the response to the disturbance. Note that a feature of this type of Green's function is that the information is sourced at one point but received by all the points. This is why it is called single-source-all-receiver Green's function, or in short, single-source Green's function (SSGF).

A tsunami is rarely triggered just at one grid point. A logical extension of this approach is to compute a group of SSGFs by placing the unit forcing successively at each of a subset of grid points, which may cover a seismic active zone. Nevertheless, when a future tsunami is triggered outside of the pre-assumed zone, the pre-calculated Green's functions would become useless. To achieve thorough hazard preparedness, one would have to include all the model grid points as potential sources. If there are  $N$  model grid points, and if the computational load for one source is a  $1 \times N$  problem, then the computational load for  $N$ -sources is a  $N \times N$  problem. When  $N$  is large, the problem becomes infeasible to tackle.

## All-Source Green's Functions (ASGF)

The all-source Green's function (ASGF) proposed by Xu (2007) focuses on a receiver point, regarding all the model grid points, including the receiver point itself, as the potential sources. The receiver point can be any point of interest (POI) for socio-economic, academic or monitorial reasons. As will become clear soon, a model run for an SSGF and a model run for an ASGF cost the same computationally, however the difference lies in their preparedness. An ASGF prepares a single POI against the entire ocean as the potential hazard sources, whereas an SSGF prepares the entire ocean against a single source point. Obviously there is no need to know how large tsunami waves will be in the middle of the oceans, whereas it is desirable that an important coastal city is prepared against the whole spectrum of tsunami sources.

With the shallow water equations in matrix form, one can now calculate an ASGF very

easily: instead of matrix-vector multiplications, he can just perform vector-matrix multiplications, as shown by the following code snippet

```

ASGF(kmax,:)=zeros(1,m+2*n); % pre-allocate memories
ASGF(1,i)=1; % a POI at i'th grid point,

for k=2:kmax % time stepping
    ASGF(k,:)=ASGF(k-1,:)*A;
end

```

So obtained  $ASGF(k,:)$  is actually the  $i$ 'th row of the dynamic matrix to the  $k$ 'th power,  $\mathbf{A}^k$ . However the algorithm avoids power calculations of the whole matrix; it only calculates for what is just needed.

In contrast with the feature of SSGF, the ASGF has a feature that the information can be sourced all over the domain but is received only at one point. This is why it is called all-source-one-receiver Green's function, or in short, all-source Green's function (ASGF). Note that the received information from the  $N$ -sources is not mixed up; the receiver has  $N$ -rooms (i.e., the  $N$ -columns) to hold  $N$ -pieces of information separately. The information will not be mixed up until a real-time event happens.

When a real-time event happens, the information stored in different rooms will be mixed up in right portions according to the actual forcing distribution. Speaking precisely, when a real-time tsunami is triggered, and if the initial tsunami distribution at the source region can be obtained by some other means, i.e., if the initial value of the  $w$ -vector,  $w^{(0)} = [\eta^{(0)} \text{ hu}^{(0)} \text{ hv}^{(0)}]^T$ , can be supplied, then the pre-calculated ASGF can be used to immediately produce a time series of the tsunami arrivals at the POI: one matrix-vector multiplication,  $ASGF \times w^{(0)}$ , takes little time to yield an arrival time series.

Comparing the above code snippets for SSAF and ASGF, one can see that the trick in switching from the SSGF to ASGF is to change the operation of the dynamic matrix on a column vector to its right side to the operation of the same dynamics matrix on a row vector to its left side. Multiplication of a row vector with a matrix costs the same as that of the same matrix with a column vector. That is why it has been said that the computational load for an ASGF is the same as that for an SSGF. The ASGF cuts down the un-needed computations for the most part of the ocean and transfers the saving to the full preparedness of a POI.

### **A Demonstrative Real-time Simulation System for Tsunami Arrivals from Anywhere in the North Atlantic Ocean**

With the ASGFs, a demonstrative system for real-time simulations of tsunami arrivals from anywhere in the North Atlantic Ocean has been developed. It is a web based system, hosted at <http://odylab.uqar.ca/tsunami>. Figure 2 shows its graphical user interface (GUI). Users can specify an arbitrary polygon as tsunami source region anywhere in the North Atlantic Ocean



by clicking on the map for the apex points of the polygon. Users can also choose one or several pre-determined POIs. After the specification, they can press the “Make plot!” button. In a few seconds a window will pop-up showing the arrival time series at the chosen POI(s). The box in the lower-left corner of the GUI shows how many seconds elapsed after the button “Make plot!” is pressed.

The system has 7 pre-calculated ASGFs for the 7 POIs offshore eastern Canada as shown by the white circular disk. More POIs could be added of course. These ASGFs are stored in hard disk in an organized way so that they can be loaded back to RAM quickly when a tsunami source region becomes known in real-time. In Figure 2, a tsunami source region is specified in the white polygon offshore African coast, and a POI for Halifax Canada on the other side of the ocean is selected. Within 7 seconds of the source specification, a pop-up window will show a 12-hours long time series of tsunami arrivals at Halifax as shown in Figure 2. The curve tells when will be the first arrival time, what will be the largest relative amplitude within 12 hours. All the details of arrivals are contained in the curve. The 12 hours period is somewhat arbitrary; it can be changed for some other reasons.

If one covers the area of the ocean by a set of tiles with size of, say  $100 \times 100 \text{ km}^2$ , for source regions, one can have a set of arrival curves at Halifax. From each of these curves, one can read off a pair of numbers, the first arrival time and the relative maximum amplitude within certain period (12 hours in the shown example). Xu (2007) defined the relative maximum amplitude driven by a small square like this as a gain. Thus, one can assign to each square a pair of number, an arrival time and a gain. Contouring the times through the squares, one can have a chart of tsunami arrival times at Halifax. Contouring the gains, one can have a gain chart as well. The time and the gain are equally important information for hazard preparedness for a POI. For examples of such charts, see Xu (2007).

The initial tsunami source function is simply assumed as follows

$$\eta^{(0)} = \begin{cases} 1, & \text{for points within the source region,} \\ 0, & \text{otherwise,} \end{cases} \quad (14)$$

$$u^{(0)} = v^{(0)} = 0 \quad \text{for all points.} \quad (15)$$

A GUI component can be added later on to allow the user to specify an arbitrary initial forcing, including non-zero initial velocities. With this feature, the system can serve a good research tool as well. For example, a geologist can specify a submarine landslide distribution based on sea bottom sonar scan data, and then to see what the response curve will be at certain POIs.

The ASGF should not be saved in a single large file. It should be chopped into many smaller ones in order to have a quick disk access when needed. One can achieve this is first by tiling the model domain, then by regrouping the columns of the ASGF such that each group of columns corresponding to a tile is saved as a small file. When a tsunami source polygon is specified, what tiles that the polygon falls into can be detected. Therefore only the ASGF files belonging to those tiles need to be read off the disk.

An equal area map projection, the sinusoidal projection, is used to for the map in the GUI, so that when a polygon is clicked for tsunami source, the area of the polygon shown on the map will be the actual area of the source region. Note the map projection is for the GUI only; the model itself does not need any map projection, since it is developed in the spherical coordinates.

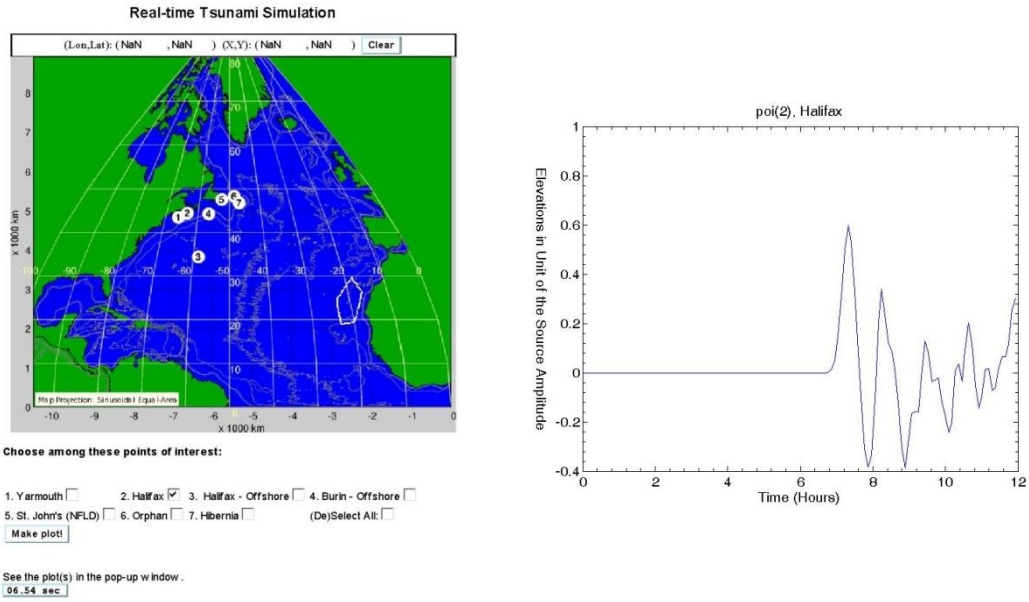


Figure 2. A demonstrative real-time simulation systems for tsunami arrivals at points of interest from anywhere in the North Atlantic Ocean is shown on the left. The POIs are located offshore eastern Canada. A white polygon offshore African coast was clicked for a tsunami source region. Within 7 seconds from the source specification, a window pops up to show the response curve at Halifax(right).

## Conclusions

Constructing global operators is rewarding. With the global operators, one can easily recast the linear shallow water equations in a matrix form. A matrix form of the shallow water equation brings in many advantages. The most significant one is that switching from the traditional single-source Green's functions to the all-source Green's function (ASGF) becomes straightforward; it is done simply by changing the column operation to a row operation. As demonstrated, the ASGF is very useful to real-time simulations of tsunami arrivals at a POI from anywhere in oceans. It transfers instantaneously a forcing anywhere to responses at a POI. If it is supplied with an initial tsunami forcing as soon as a tsunami is triggered, the ASGF can provide a local run-up model immediately with nearshore open water boundary conditions. This will help the local run-up model to have sufficient time to simulate possible inundation scenarios, providing disaster mitigation decision makers with sounding information.

An initial tsunami forcing should directly come out of a tsunami generation model. However in case it is difficult to do so, the ASGF can be of help to indirectly estimate the initial forcing: Let the ASGFs be pre-calculated for a set of tsunami monitoring stations (such as the

DART mooring system, <http://nctr.pmel.noaa.gov/Dart/about-dart.html>), when tsunami signals arrive at these monitoring stations, the pre-calculated ASGFs can be used, as in an inverse problem, to infer the initial conditions at a source region.

If a real-time arrival simulation system can be established for the North Atlantic Ocean, so it can be for the whole world ocean. A global coverage may require billions of grid points; however the number of important coastal cities worldwide is a very small number compared with the huge number of the grid points. It is thus feasible to pre-calculate the ASGFs for the worldwide important coastal cities.

The demonstrated North Atlantic system is web-based. To cut down the time needed to travel through the internet, the system can be made on a local desktop. Every local emergency manage officer (EMO) should have such a tool in their office. When a real event happens, and even if the initial forcing cannot be obtained in time, the system still can tell the EMOs the time and maximum relative amplitude. It will make EMOs a significant difference in responding if they can be told the gains in their coasts are less than 10% or more than 90% of the largest ever possible waves in a source region.

### **Acknowledgments**

Mr. Michel Beaulieu is acknowledged for his helping with the <http://odylab.uqar.ca/tsunami> and so is University of Quebec at Rimouski for hosting the web page. The author also wishes to thank Ms. Alana Stobert for proof-reading the manuscript.

### **References**

- Arakawa, A., and V. R. Lamb, 1977. Computational design of the basic dynamical process of the UCLA general circulation model. *Methods in Computational Physics*. 17, Academic Press, 173-265.
- Chapman D. C. 1985. Numerical Treatment of Cross-Shelf Open Boundaries in a Barotropic Coastal Ocean Model. *Journal of Physical Oceanography*, 15:8, 1060-1075
- Heaps N. S. 1969. A Two-Dimensional Numerical Sea Model. *Philosophical Transactions for the Royal Society of London. Series A, Mathematical and Physical Sciences*, Volume 265, Issue 1160, pp. 93-137
- Shuto N. 1991. Numerical Simulation of Tsunamis --- Its Present and Near Future. *Natural Hazards* 4: 171-191.
- Sommerfeld A. 1949. *Partial Differential Equations in Physics*. Academic Press, New York, New York, 1949.
- Xu Z. 2007. The all-source Green's function and its applications to tsunami problems. *Science of Tsunami Hazards*, 26(1), 59-69.